Heliyon 10 (2024) e24260

Contents lists available at ScienceDirect

Heliyon

journal homepage: www.cell.com/heliyon

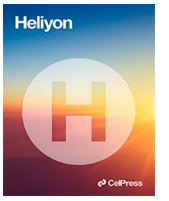

Research article

Development and characterization of non-proprietary ultra high performance concrete

Muhammad Azhar Saleem [a], Faizan Liaquat [a], Muhammad Mazhar Saleem [a], Mubashir Aziz [b,c], Fahid Aslam [d,*], Abdullah Mohamed [e]

[a] Department of Civil Engineering, University of Engineering and Technology Lahore, Lahore, Pakistan
[b] Department of Civil and Environmental Engineering, King Fahd University of Petroleum and Minerals, Dhahran, Saudi Arabia
[c] Interdisciplinary Research Centre for Construction and Building Materials, King Fahd University of Petroleum and Minerals, Dhahran, Saudi Arabia
[d] Department of Civil Engineering, College of Engineering in Al-Kharj, Prince Sattam bin Abdulaziz University, Al Kharj, 11942, Saudi Arabia
[e] Abdullah Mohamed Research Centre, Future University in Egypt, New Cairo, 11835, Egypt

ARTICLE INFO

Keywords:
Ultra high performance concrete
UHPC
Non-proprietary
Low-cost
Characterization

ABSTRACT

This paper presents the developmental process of ultra-high performance concrete (UHPC), the most advanced form of concrete. The entire process exclusively utilized locally available materials. The mixes were prepared without using any specialized mixer or treatments, such as elevated pressure, etc. The primary objective of the research was to develop low-cost non-proprietary version of UHPC by optimizing both cementitious and non-cementitious materials to attain the highest levels of workability, compressive strength, flexural strength and durability. The research utilizes a trial-and-error approach, subjecting specimens to curing in both regular and heated water. The findings validate the viability of producing self-compacting UHPC with compressive strength ranging from 120 to 160 MPa, employing local materials and manufacturing methods. Raw materials and mixing sequence had a significant influence on the fresh and hardened properties of UHPC. The inclusion of steel fibers and the application of heat treatment remarkably enhanced the compressive strength. Furthermore, cost analysis revealed that this particular UHPC is only slightly over four times more expensive than conventional concrete, in contrast to commercially available UHPC, which is approximately 10 times expensive than traditional concrete.

1. Introduction

Ultra high performance concrete (UHPC) is defined as hydraulic cement-based concrete, which has excellent mechanical and durability properties, minimum water-to-binder (W: B) ratio, and extremely dense structure having virtually zero porosity, resulting in high resistance against severe environmental conditions. This newly developed fiber reinforced concrete is usually described by its compressive strength ranging from 120 to 150 MPa (around seven times higher than conventional concrete). Swiss Standard specifies 120 MPa as the minimum compressive strength, Frech and German Standard specify a strength of 130 MPa, whereas Japanese Standard and ACI 239R-18 specify a minimum compressive strength of 150 MPa. ACI 239R-18 specifies that UHPC has a direct tensile strength in the range of 6–12 MPa and a modulus of elasticity of 40–50 GPa. Also, UHPC has nominal creep and a maximum packing

* Corresponding author.
E-mail address: f.aslam@psau.edu.sa (F. Aslam).

https://doi.org/10.1016/j.heliyon.2024.e24260
Received 17 October 2023; Received in revised form 2 January 2024; Accepted 5 January 2024
Available online 8 January 2024

density, which makes it nearly impermeable to the ingression of water, sulfates chlorides, etc. It is reinforced with steel or other high-performance fibers to achieve ductility. The ultra-high compressive strength of UHPC significantly minimizes the section size thus UHPC structures are one-third to one-half lighter than their traditional concrete counterparts under similar loading conditions. Its superior durability results in extended service life and reduced maintenance cost. The increased abrasion resistance offers long service life to industrial floors and bridge decks, whereas increased corrosion resistance ensures durability in highly humid weather [1–3].

UHPC is a blend of different types of concretes, commonly known as self-compacting concretes (SCC), high-performance concretes (HPC), and fiber reinforced concretes (FRC) [4,5]. Bouygues was the pioneer, who investigated Reactive Powder Concrete, a kind of UHPC, during the years 1990–1996. Although no clear definition of UHPC exists in the open literature and no widely accepted standard has been developed yet for preparing UHPC but still, it has gained popularity in structural applications [6]. The Sherbrooke pre-stressed footbridge constructed in Canada in 1997 was the world's first engineering structure designed and constructed with UHPC. During the years 1997 and 1998, UHPC was used in the first industrial application in Cattenom and Civaux power plants for replacing cooling tower's steel beams. The world's first UHPC bridges were realized at Bourg-les-Valence in France during the years 2000–2001 [7].

Commercially available ready mix UHPC such as Ductal®, BSI®, and CEMENTE are 10–20 times more expensive than regular concrete, which deters its widespread use [8]. Since its launching in the commercial market in 1995, UHPC has been under detailed exploration around the world [7,9–18]. Several researchers around the globe have developed UHPC utilizing conventional raw materials and production techniques as summarized in Table 1.

The primary objective of this work was to develop non-proprietary UHPC characterized by exceptional flowability and a compressive strength exceeding 150 MPa, utilizing locally sourced raw materials and common technology. This has the potential to significantly lower the production costs associated with UHPC. The term "non-proprietary" implies that the mix design and preparation process are openly accessible for anyone wishing to replicate this UHPC, in contrast to commercial products available only in ready-mix form, with undisclosed proportions and preparation methods.

2. Raw material

Ingredients included ordinary Portland cement (OPC), coarse sand, silica sand, silica fume (SF), quartz powder, super-plasticizer (SP), steel fibers, and water. Ground granulated blast furnace slag (GGBFS) was also used as a partial replacement for cement in a few mixes. Details of each constituent are summarized in subsequent sections.

2.1. Portland cement

Commercially available cement from three different sources was used and named CEM-I, CEM-II, and CEM-III (Table 2). These types of cement conform to PS: 232–2008 (R) [22] equivalent to ASTM C 150/Type I [23] and have a low Blaine fineness and a low C_3A content, to have a high amount of C_3S and C_2S. Fig. 1 shows the XRD pattern of a representative specimen of the cement powder. As expected, tricalcium silicate ($3CaO{\cdot}SiO_2$), otherwise known as alite is a major phase in the OPC. Phases of calcium carbonate ($CaCO_3$) and silicon dioxide (SiO_2) can also be identified, though quantitatively not very dominating. The oxides of Al, Fe, K, etc are the weaker phases. The average crystallite size of the OPC powder is nearly 40 nm. According to the manufacturer's note, the cement contains 95 % clinker, and 5 % gypsum and can attain compressive strength up to 69 MPa after 28 days. Table 2 illustrates the physical properties of all types of cement. The chemical composition of the oxide phases in the cement is presented in Table 3.

2.2. Coarse sand

Lawrencepur sand with a fineness modulus of 2.72 was used. This sand is relatively coarser. Therefore, it was used after sieving through a 4.75 mm sieve and excluding very coarse particles such as small stones larger than 5 mm. The loose bulk density and rodded bulk density of this sand were 1640 kg/m^3 and 1755 kg/m^3, respectively.

2.3. Silica sand

The quartz sand was acquired from the Kamar Mushani town of Mianwali District. It was yellowish-white in color. As per chemical analysis, silica content (SiO_2) was more than 98 % and the remaining 2 % consisted of Al_2O_3, Fe_2O_3, TiO_2, CaO, MgO, K_2O, Na_2O. Its particle size was within the range of 0.06–2.00 mm.

Table 1
UHPCs developed by various researchers.

Researcher	Year	Country	Raw material	Specimen shape	Compressive strength (MPa)
Katrin et al. [19]	2008	Canada	Local	Cube (50 mm)	125 MPa
Allena et al. [20]	2010	Mexico	Local	Cube (50 mm)	165 MPa
Wang et al. [7]	2012	China	Local	Cube (100 mm)	180 MPa
Sobuz et al. [21]	2016	Australia	Local	Cylinder (100 mm)	153 MPa
Alsalman et al. [3]	2017	USA	Local	Cube (50 mm)	155 MPa

Table 2
Physical properties of cement.

Cement brand		CEM-I	CEM-II	CEM-III
Compressive strength	3 Days (MPa)	30.5	43.5	41.4
	7 Days (MPa)	37.5	54.2	48.7
	28 Days (MPa)	50.6	69.2	70.2
Setting time	Initial (min)	205	150	150
	Final (min)	270	200	200
Soundness (mm)		0.5	1.0	1.0
Fineness (m^2/kg)		328	336	315

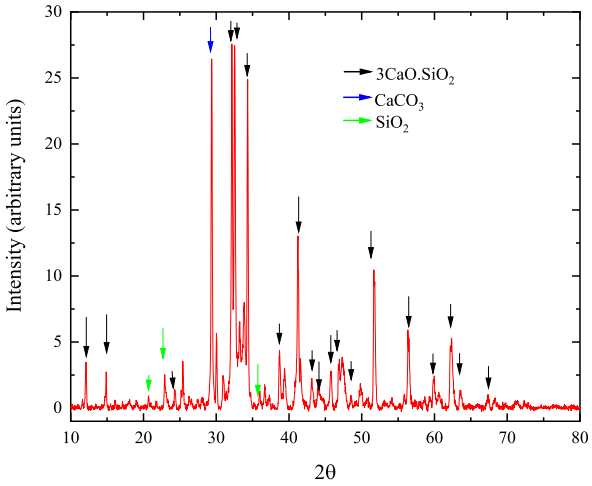

Fig. 1. XRD pattern for the OPC powder.

Table 3
Portland cement composition.

Composition (wt. %) of Portland Cement	
SiO_2	20.97 %
Al_2O_3	4.16 %
Fe_2O_3	5.55 %
CaO	63.57 %
MgO	1.01 %
SO_3	1.91 %
Na_2O	0.17 %
K_2O	0.46 %

2.4. Silica fume (SF)

Silica fume mainly comprises spherical particles of silicon dioxide having Blaine fineness of 20,000 m^2/kg and size smaller than 10 to 6 μm. According to Norchem (2017), It is highly pozzolanic. Silica fume reacts with calcium hydroxide (CH) and produces calcium silicate hydrate (CSH), which not only provides improved compressive, flexural, and bond strength but also results in a much denser matrix and high durability. Monteiro (1990) observed that blended water reduction as well as the pozzolanic reaction of silica fume and CH reduces the thickness of the Interfacial Transition Zone (ITZ). In the current work, commercially available dark grey color densified SF marketed under the brand name of Master Roc® MS 610 and manufactured by BASF Chemicals® was used.

2.5. Quartz powder

Cwirzen (2006) stated that quartz remains inert at room temperature and mostly acts as a filler to improve the packing density of the concrete. Its particle size is between 5 and 100 μm. At higher temperatures, it gets activated and consumes portlandite through pozzolanic reactions. This reaction increases the compressive strength if quartz is used in the right proportions with respect to cement. Quartz powder was acquired from a local brand named Imporient Chemicals®. It is usually used for preparing high-strength grouting material in Pakistan. Quartz powder was in yellowish-white color.

2.6. Ground granulated blast furnace slag (GGBFS)

GGBFS was supplied by Steel Mills, Karachi. It was in the form of small stones, which could not be used directly in concrete preparation. Therefore, it was ground in a flour crusher to obtain a finely grounded form to activate pozzolanic action. It was used for the partial replacement of cement. The XRD pattern of GGBFS as shown in Fig. 2, illustrates a hump from 25° to 35° shows the slab is largely made up of amorphous compounds and that no significant crystalline phases were present. However, a sharp peak appearing at 29.3° from sylvite (KCl) is visible.

2.7. Admixtures

Locally available third-generation superplasticizers (SPs) supplied by two different manufacturers were used. All SPs were poly-carboxylate ether (PCE) based. The technical data of SPs are presented in Table 4. The accelerator used in the mix trials was Rheocrete CNI provided by BASF®.

2.8. Steel fibers

According to Cwirzen (2006), fibers mainly help induce ductile behavior and enhance flexural strength by bridging cracks. Incorporation of 11–32.5 % of steel fibers by the weight of cement enhances the compressive strength by 18.2 %, tensile strength by 66.1 %, and flexural strength by 40 %. Also, for a constant diameter, longer fibers (l/d = 50) increase compressive and flexural strengths slightly more than shorter fibers (l/d = 30) (Hamdy K, 2016). Compressive strength or the modulus of elasticity of UHPC is not very sensitive to the alignment of fibers, however, flexural strength is. Two types of straight steel fibers as shown in Fig. 3 were used. Their basic characteristics are presented in Table 5.

2.9. Water

Potable drinking water was used for preparing all the UHPC mixes and for curing.

3. Mix design optimization

The optimization of the mix for UHPC results in the minimization of voids like micro-cracks and pores that help to attain higher strength and improved durability characteristics [24]. In the current study, the design of the UHPC mix using the hit and trial method was aimed at obtaining a densely compacted cementitious matrix having excellent flowability and compressive strength. Hit and trial means that all the mix proportions were not cast at the same time. Only 2 to 3 mixes were cast together and based on their results the proportions for the subsequent mixes were finalized. This process of optimization helped in determining the most economical and practical combination of concrete ingredients that was workable in its plastic state and developed the required characteristic when hardened. To obtain a dense matrix with very low permeability, the maximum grain size had to be controlled, along with the cement content, W: B ratio, SP dosage, steel fibers fraction, and the curing method. Currently, there is no international code for designing the mix of UHPC, therefore trial methods are commonly used. ACI 239R-18, however, provides some basic guidelines about the materials and production of UHPC. This report presents two possible UHPC mixes identifying the ratios of various constituents. For instance, the steel fiber content by mass of cement is proposed as 0.20 and 0.31 for mixture proportions 1 and 2, respectively.

To save efforts and expensive materials, instead of carrying out trials from ab-initio, a previously used mix [24] which can produce

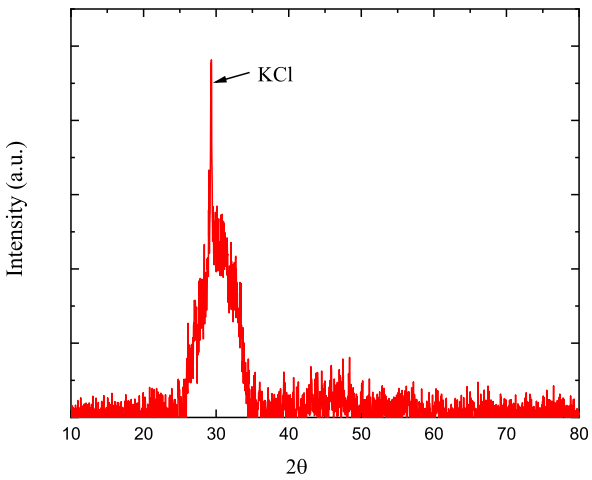

Fig. 2. XRD pattern for GGBFS.

Table 4
Technical data of selected super-plasticizers.

SP brand	SP-I	SP-II
Type	PCE based	PCE based
Color	Amber	Whitish pale
Density (kg/lit)	1.082–1.142	1.06 ± 0.01
Chloride content (%)	<0.1	Nil

Fig. 3. Long straight steel fibers.

Table 5
Features of selected steel fibers.

Steel fibers	Short Steel Fiber (SSF)	Long Steel Fiber (LSF)
Type	Short	Long
Diameter (mm)	0.3	0.5
Length (mm)	19.5	32.5
Aspect ratio	65	65
Density (kg/m^3)	7850	7850

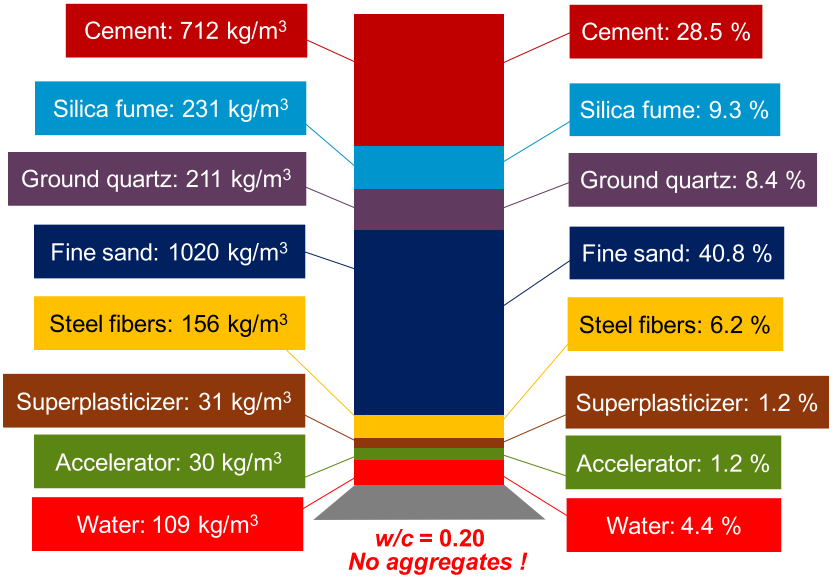

Fig. 4. Reference mix design [14].

Table 6
Trial mixes of UHPC.

Category	UHPC mixture	ID	Binder (kg/m^3)	Sand (kg/m^3)	QP (kg/m^3)	GGBFS (kg/m^3)	SP (kg/m^3)	Accelerator (kg/m^3)	Steel fibres (kg/m^3)	Water (kg/m^3)	W:B Ratio	Curing regime
A	1	CEM-I, SP-I,SSF	943	1020	211	–	30.7	30	156	109	0.19	Nil
	2	CEM-I, SP-II, SSF	939	1020	211	–	30.7	–	156	143	0.2	NC
	3	CEM-I, SP-II, SSF	986	1020	211	–	30.7	30	50	173	0.18	NC
	4	CEM-I, SP-I,SSF	981	1020	211	–	30.7	30	75	153	0.19	NC
B	5	CEM-I, SP-I	718	1020	210	238	45	30	–	239	0.25	NC
	6	CEM-I, SP-II	945	937	167	168	31	30	–	222	0.2	HC
	7	CEM-III,SP-II, SSF	758	979	210	225	30.7	–	100	197	0.2	HC
	8	CEM-III,SP-I, LSF	834	972	210	150	37.5	–	100	197	0.2	HC
C	9	CEM-III,SP-II, SSF	984	979	210	–	30.7	–	100	197	0.2	HC
	10	CEM-III,SP-II, SSF	984	979	210	–	30.7	–	100	197	0.2	HC
	11	CEM-III,SP-II, LSF	984	979	210	–	30.7	–	100	197	0.2	HC
	12	CEM-III,SP-I, LSF	984	950	210	–	59.2	–	100	197	0.2	HC
	13	CEM-III,SP-I, LSF	984	965	210	–	45	–	100	197	0.2	HC
	14	CEM-II, SP-I,LSF	984	972	210	–	37.5	–	100	197	0.2	HC
	15	CEM-II, SP-II, LSF	984	972	210	–	37.5	–	100	197	0.2	HC
	16	CEM-II, SP-I,LSF	984	992	210	–	37.5	–	100	177	0.18	HC
	17	CEM-III,SP-I, LSF	984	972	210	–	37.5	–	100	197	0.2	HC
	18	CEM-III,SP-II, LSF	984	972	210	–	37.5	–	100	197	0.2	HC
	19	CEM-III,SP-I, LSF	984	986	210	–	43.5	–	100	177	0.18	HC
	20	CEM-III,SP-II, LSF	984	922	210	–	37.5	–	150	197	0.2	HC
	21	CEM-II, SP-II, LSF	1032	861	210	–	40	–	150	207	0.2	HC
	22	CEM-II, SP-I,LSF	1032	861	210	–	40	–	150	207	0.2	HC
	23	CEM-II, SP-I,LSF	1032	859	210	–	42.5	–	150	207	0.2	HC
	24	CEM-III,SP-II, LSF	1032	859	210	–	42.5	–	150	207	0.2	HC
	25	CEM-III,SP-II, LSF	1082	799	210	–	42.5	–	150	217	0.2	HC

strength close to 150 MPa was selected from the literature (Fig. 4). The choice of materials was based on the particle size to effectively occupy the matrix voids and to achieve a compact microstructure. Owing to the absence of coarse aggregate, the sand, with the largest ratio in the mixes. Followed by the Cement, Quartz, and then silica fume.

All the mixes were tested for workability and compressive strength. The 100 mm cubes were used for the compression test. A total of 350 cubes were prepared for various mix designs. For each category of the mix, five cubes were tested to observe variations in the characteristic compressive strength.

The whole process of optimization was completed with three different types of cement, one type of silica fume, two types of sand, and three different types of super-plasticizers. The content of ingredients of the reference mix and curing regimes were kept on changing to check and, if suitable, optimize the previous mix design. The entire stock of mixes was divided into three categories. The details of the mixes are given in Table 6. Table 6 presents some selected mix designs only otherwise, many other mix designs were also investigated. The mixes were categorized as follows:

Category A: The reference mix was used in this category by incorporating cement CEM-I and short steel fibers (SSF). The content of ingredients as well as the W: B ratio was also kept on changing. The dosage of the super-plasticizer was kept constant. The super-plasticizer SP-I and SP-II were used in these mixes. Some mixes were developed without accelerators and steel fibers to check if these were necessary for achieving the desired properties and to see if the mix could be economized by eliminating these two ingredients. It was observed that there were no issues with setting time, therefore, the use of the accelerator was discontinued in all subsequent mixes. Steel fibers have a significant influence on mechanical properties other than compressive strength, therefore, they cannot be eliminated. After testing, it was concluded that CEM-I and SSF are not suitable for the development of UHPC. The maximum compressive strength obtained in this category was about 95 MPa.

Category B: The GGBFS was used in this category for the partial replacement of cement. The content of ingredients as well as the W: B ratio was varied among mixes. Two mixes of this category were developed with the accelerator, however, these were discontinued because there were no issues with setting time. In the initial few mixes, steel fibers were not used. However, the remaining mixes of this category incorporated steel fibers. Two types of cement CEM-I and CEM-III were used in these mixes. The results concluded that the performance of CEM-III is manifold better than that of CEM-I and it can produce UHPC with compressive strength higher than 150 MPa.

Category C: The reference mix with some variations was used in this category. The cements CEM-I, CEM-II, and CEM-III; super-plasticizers SP-I, and SP-II; and both types of steel fibers were used in this category. The content of cement, steel fibers fraction, and SP dosage were the variables. However, the silica fume and quartz powder content as well as the W: B ratio were kept constant in almost all mixes. Optimization results confirmed that CEM-II and CEM-III are the best types of cement for producing UHPC with a low W: B ratio of 0.20. The mixes of this category resolved the compatibility issues between different types of cement and superplasticizers and provided the optimum SP dosage necessary for producing a self-compacting UHPC mix. The use of SP-I was discontinued for future research because it failed to maintain the low W: B ratio. The use of SSF was discontinued at an early stage. Moreover, the steel fibers with a 2 % volume fraction were found to be appropriate both in terms of mechanical performance and economy. The above-mentioned findings of this category helped in achieving compressive strengths within the desired range i.e. 120-150 MPa.

Table 7 provides the final proposed mix which is economical and workable, and can achieve compressive strength above 150 MPa. This will be called the optimized mix. The W: B ratio and water-to-cement ratios were determined as 0.20 and 0.26, respectively. The amounts of silica fume and quartz powder are 29 % and 26 %, respectively by weight of cement, and that of superplasticizer is 4.1 % by weight of the binder amount. The optimum dosage of steel fibers is 2 % by volume of UHPC, or around 156 kg/m^3. Also, CEM-III, SP-II, and LSF are the most suitable.

4. Mixing regime

An ordinary pan type mixer with a capacity of 0.057 m^{3}as shown in Fig. 5 was used. This vertical axis mixer was a little under-powered for such an application, leading to prolonged mixing times in comparison to high shear mixers generally used for producing

Table 7
Optimized mix design of UHPC.

Constituent	Mix Design	
	kg/m^3	Ratio
Cement	800	1
Fine sand	430	0.54
Silica sand	430	0.54
Silica fume	233	0.29
Quartz powder	210	0.26
GGBFS	–	–
Quartz stone	–	–
Superplasticizer	42.5	0.05
Accelerator	–	–
Steel fibers	150	0.19
Water	207	0.26
W:B Ratio	0.2	0.2

UHPC. The mixing procedure, as recommended in reference no. 14, was followed with some modifications [24]. The step-wise mixing scheme is described below.

- Step 1: All the powders were dry mixed for 5–10 min at low speed.
- Step 2: All water premixed with half SP was then added slowly for 2 min and mixing continued for approximately 10 min (5 min with a low speed and 5 min with a high speed)
- Step 3: The remaining half of SP was added and mixing proceeded at a high speed until UHPC changed to a fluid state
- Step 4: Steel fibers were gradually added over the span of 2 min and then mixing continued at a high speed until uniform distribution of fibers was achieved.

This sequence of mixing enabled the SP to become fully effective and a consistent mix was reached every time. The mixing times from steps (3 & 4) were varied among mixes due to the use of different types of cement and super-plasticizer. This variation was from 2 to 6 min for steps (3 & 4) to bring the workability to the desired level.

Total mixing time was 15–20 min for a few initial mixes due to compatibility issues between different types of cement and super-plasticizers. The total mixing time never exceeded 20 min. The entire mixing process took about 12–15 min for the optimized mix.

5. Casting of specimens

The specimens were cast in molds in two equal portions. Vibrations were not applied. All specimens were slightly compacted by tapping outside the molds (Fig. 6). The samples were de-moulded after 24 h the sand was transferred to a curing tank.

6. Curing regime

Two curing methods were followed: normal curing (NC) and heated curing (HC). In NC, concrete cubes were immersed in water at a room temperature of 25 $\pm$ 2 °C till the day of the testing day. For the HC, the specimens were initially cured in nearly boiling water for 48 h and then NC was applied until the day of testing. NC was used only for a few initial mixes. Later on, heated curing was used for all the mixes. A local household burner was used for carrying out heated curing. The specimens were kept in a small steel container as shown in Fig. 7. The type of curing regime adopted for any particular mix is provided in Table 6.

7. Experimental methods

7.1. Workability

The slump flow (Fig. 8) of all UHPC mixes both with and without steel fibers was measured in accordance with ASTM C1611/

Fig. 5. Ordinary pan type mixer.

Fig. 6. Casting of UHPC specimens.

Fig. 7. Specimens under heat curing in a steel container.

1611M − 14 [25]. The cone was filled with concrete in a single step without any tamping or vibration. Any surplus concrete was removed from around the base of the concrete. After this, the cone was lifted straight upwards to avoid any jolting, and the concrete was allowed to spread outward freely. Once the concrete reached a steady state, two diameters (d_1 and d_2) of the concrete mass were measured in orthogonal directions. The average of the two (eq. (1)) measured diameters was reported as the slump flow in mm.

$$\text{Slump flow} = (d_1 + d_2) / 2 \tag{1}$$

Fig. 8. Slump flow measurement of optimized mix.

where:

d_1 = Largest diameter of the circular spread of the concrete

d_2 = Spread of the concrete at an angle perpendicular to d_1

7.1.1. Compressive strength

The compressive strengths of all 100 mm cube specimens were determined with standard procedures conforming to the British Standard EN 12390–3:2001 [26]. Cubes were preferred over cylinders to avoid concerns related to ends' preparation. Five cubes were replicated for each age for the trial mixes and three cubes for the optimized mix. The specimens were tested using a compression testing machine with a maximum load capacity of 3000 kN. Loading was applied at a uniform rate without any shock until the specimen failed.

After arriving at the optimized mix, the compressive strength of cylinders of size 75 mm × 150 mm was also investigated following ASTM C39 [27], in addition to cube specimens. Compression testing of each mix was undertaken at the age of 7 and 28 days to quantify the rate of gain of strength. A few mixes were also tested at the age of 14 days.

7.1.2. Flexural strength

The flexural performance of UHPC was examined using prisms measuring 100 mm × 100 mm × 500 mm, in accordance with ASTM C78-02. The flexural strength was determined by subjecting a simply supported beam to third-point loading using a strain-controlled universal testing machine. A displacement rate of 1 mm/min was employed, with loading applied steadily until fracture occurred. This flexural strength test was conducted on ten specimens at 28 days of age. The initial crack load and peak load were recorded, and the findings were reported as the modulus of rupture.

7.1.3. Sulphate resistance

The sulphate resistance test was conducted on UHPC specimens measuring 100 mm × 100 mm × 100 mm in accordance with ASTM C1202. Sodium sulphate was selected as the sulphate source. A total of twelve specimens were subjected to sulphate exposure. Following 28 days of curing, all specimens were fully immersed in steel containers containing different concentrations of sodium sulphate (Na_2SO_4) solutions, specifically 1 % and 5 %, for 56 days. Here, a 1 % sodium sulphate solution denotes a mixture of 1 % sodium sulphate and 99 % water. The concentration of sodium sulphate was increased from 1 % to 5 % after the initial 28 days of exposure. To ensure consistent concentration, the sodium sulphate solutions were stirred weekly and replaced at least monthly or when cloudiness was observed. Periodic visual inspections were carried out to monitor the physical condition of the specimens, including aspects such as scaling, chipping, and crack patterns. At intervals of 7, 14, 28, and 56 days of exposure, three specimens each were extracted from the container to assess the impact of sulphate attack in terms of changes in length and mass, as well as the loss of compressive strength.

8. Results and discussion

8.1. Workability

Slump flow results with and without fibers are shown in Fig. 9. Slump flow ranged from 475 to 780 mm. This wide range can be attributed to the use of cement and super-plasticizer from different sources. The slump flows for most of the mixes except a few were within the EFNARC [28] range for self-compacting concrete i.e. 650 mm − 800 mm. However, the slump flows of nearly all the UHPC

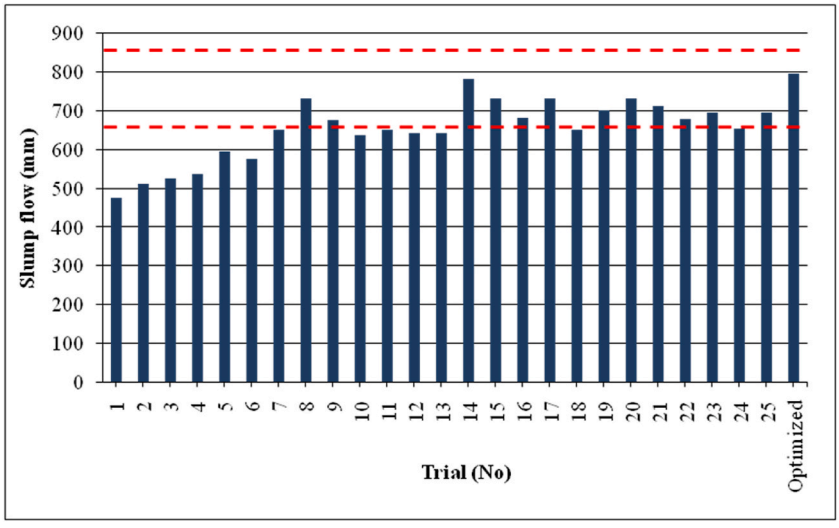

Fig. 9. Summary of slump Flow for all the mixes.

mixes were in the range of the European Guidelines [29]for self-compacting concrete i.e. 550 mm–850 mm. Therefore, these UHPC mixes can be treated as self-compacting. The optimized mix yielded a slump flow value of 795 mm.

8.1.1. Effect of cement

The results indicated that cement is the most crucial element in the mix design regarding workability. All the mixes made using CEM-I exhibited slump flow values lesser than 600 mm, which are also lesser than their counterparts prepared with CEM-II and CEM-III. These results are comparable with the previous studies [30,31] where the cement constituents were similar as reported in this work. Although, a slump flow value of 690 mm was recorded previously [32] with smaller cement and steel fiber contents than those of this report, however, those specimens included a significant amount of fly ash (around 1286 kg/m^3). It was noted that the flow increased slightly at the same W: B ratio when CEM-II was used instead of CEM-III and CEM-I. This slight increase in the case of CEM-II was due to lower water absorption and smoother surfaces of particles. It can be concluded from the workability results that the water demand for different types of cement lies in the decreasing order of CEM-II < CEM-III < CEM-I. It was also observed that the slump flow difference between CEM-II and CEM-III is very small. Therefore, both CEM-II and CEM-III are suitable for preparing self-compacting ultra high performance concrete at a very low W: B ratio.

8.1.2. Effect of supplemental materials

It is clear from the results that the effect of using SF with cement was positive on the workability of the mixes which is also consistent with the previous studies [32–34]. The absence of SF causes slum flow to decrease significantly, up to 355 mm [34]. This can be attributed to the spherical nature of SF particles, which helps in lubrication. The results confirmed that all selected supplementary cementitious materials performed suitably for UHPC design except GGBFS, which negatively influenced the workability.

8.1.3. Effect of binder content

The optimized mix of UHPC with 1033 kg/m^3 binder presented a very good fluidity with a slump flow of 795 mm, which is three times better than the previously reported [35] value of 250 mm with a W: B ratio of 0.22. Therefore, it is important to maintain high paste volume to achieve high workability and ultra-high strength. In this study, 1033 kg/m^3 binder was set as the ceiling to maintain a balance between performance (workability and compressive strength) and cost.

8.1.4. Effect of super-plasticizer

SP-II outperformed the other SPs utilized in this research. SP-I demonstrated compatibility issues with all selected types of cement even at a higher dosage. It resulted in the setting of the matrix very quickly (3–5 min) after mixing. Because of the inferior workability of the paste with SP-I, this SP is not appropriate for the mix design of UHPC. The SP dosage was adjusted to ensure that the slump is maintained between 650 and 800 mm, which enables the mixes to be self-compacting. The specimen showing higher values of slump flow had an SP content of 37.5 kg/m^3 or higher. This quantity is significantly smaller than 200 kg/m^3, which resulted in a slump flow of 600 mm [34]. Further, the slump flow values reported in this work are better than the values reported with almost the same amount of SP contents reported previously [26,32,33]. The results showed that cement requires more SP to obtain the desired slump flow compared to other cementitious materials. The amount of super-plasticizer increased with the increase in the amount of cement. It was concluded that the optimum SP dosage for 1 kg of cement is 0.05 L. Moreover, it was observed that the step by step addition of SP significantly enhanced uniform dispersion and consequently workability.

8.1.5. Effect of steel fibers

Slump flow was significantly influenced by the fiber length and dosage. It was observed during mixing that the inclusion of fibers

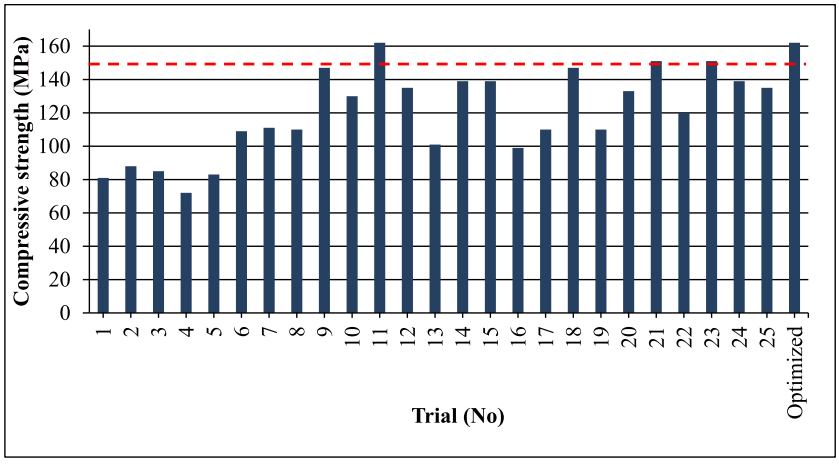

Fig. 10. Summary of compressive strength for all the mixes.

negatively affected the workability of the fresh concrete. The workability loss of concrete with the addition of fibers may be attributed to the increased friction due to the entangling of fibers and the cohesion of fibers with other ingredients. Similar findings were reported in the literature [35]. Although the inclusion of steel fibers reduced the slump flow, workability was brought to the desired level in all UHPC mixes either by the additional mixing time or in some cases by increasing the dosage of SP.

8.1.6. 6Effect of concrete mixer

The desired workability and compressive strengths were achieved without using a high-shear mixer. However, due to the low power of the mixer, the total mixing time required for the UHPC to reach adequate workability and consistency was increased to around 15 min, however, no negative effects of increased mixing time were observed.

8.2. Compressive strength

The average compressive strength results of all the UHPC mixes at 28 days are presented in Fig. 10. The finally proposed optimized UHPC mix achieved an average compressive strength of 162 MPa after 28 days, with a confidence level of 95 %. The standard deviation was 4 MPa and the coefficient of variation was 2.7 %. The compressive strength of all the mixes fluctuated between 72 and 162 MPa. In general, the mixes showing high slump flow also exhibited high compressive strength. For example, the UHPC mix 20 (Table 6, CEM-III, SP-II, LSF), exhibited slump flow higher than 700 mm and compressive strength of 150 MPa. Similarly, mix 11 which showed a compressive strength of 162 MPa, had a slump flow of almost 650 mm.

8.2.1. Effect of cement

The results demonstrated that cement is the most crucial ingredient regarding workability and strength development. The highest compressive strength values were achieved by CEM-III, followed by CEM-II and CEM-I. It was found that CEM-I is not suitable for preparing ultra high performance concrete however, its strength was in the range of 85–100 MPa which is still higher than ordinary concrete. This result is most likely explained by the composition of CEM-I, which has a combination of a high C_3A content ($C_3A = 4$ %, responsible for the decrease in strength) and a low C_3S content ($C_3S = 74$ %, responsible for the increase in strength). However, CEM-II ($C_2S = 16$ %, $C_3S = 60$ %) and CEM-III ($C_2S = 10$ %,$C_3S = 60$ %) achieved comparable strength because they had similar C_2S and C_3S contents. Results confirmed that pastes with a cement of low Blaine values and high in $C_3S + C_2S$ perform best for strength development.

To study the impact of varying cement quantities on the compressive strength of UHPC and determine the optimum cement content, a few trial batches were developed by making use of different amounts of cement including 725, 750, 800, and 850 kg/m^3. It should be mentioned that, in this case, the total W: B ratio and the super-plasticizer/cement ratio were kept constant. As expected and consistent with the previous observations [32,34,36], the compressive strength of the concrete increases by increasing the content of cement. It should be particularly noted that the specimens meeting the threshold compressive strength of 150 MPa had binder contents of 984 kg/m^3 or 1032 kg/m^3 which is almost 30 % less than the previously reported [37] value of 1543 kg/m^3. Results further revealed that a cement quantity of 750 kg/m^3 utilized in the optimized mix resulted in a maximum compressive strength of 162 MPa.

8.2.2. Effect of water-to-binder ratio

Decreasing water content increased the UHPC compressive strength. The optimized mix design was obtained by using a minimum W: B ratio in agreement with the literature [3,34,37]. The main reason behind this phenomenon is that the effective hydration of cementitious materials requires an optimum and determined amount of water without leaving any extra water in UHPC. The use of excess or less water than the optimum amount negatively influences the compressive strength of UHPC. The optimized W: B ratio was determined as 0.20, which led to maximum compressive strength.

8.2.3. Effect of supplementary materials

It is well known that supplementary materials affect the compressive strength of the concrete both positively and negatively [38]. It is important to establish the optimum amount of supplementary materials [39–41]. The specimens with the sand and steel fibers quantities of 972 kg/m^3 and 100 kg/m^3, respectively exhibited the highest compressive strength. In addition, optimized quantities of sand, QP, and SP are 922 kg/m^3, 210 kg/m^3, and 37.5 kg/m^3, respectively. Fardis [38] stated that the compressive strength improves with the increase in the quantity of SiO_2. This is because of the replacement of Calcium Hydroxide $Ca(OH)_2$ which has lesser strength than Calcium Silicate Hydrates (CSH), which possess much greater strength. CSH is produced in the chemical reaction between $Ca(OH)_2$ and pure SiO_2. This pure SiO_2 was available because of using silica fume, quartz sand, and quartz powder, which are the major forms of pure silica that exist naturally. Since there was no coarse aggregate in UHPC, there were fewer cavities in it, resulting in higher strength of UHPC.

8.2.4. Effect of curing method

The curing method applied to the UHPC had a significant effect on the compressive strength. Heated curing played a role in the strength development of each mix. It was observed that if other conditions remain similar, the compressive strength of UHPC under heated curing was on average 24 % greater than normal curing. It was because of the speedy pozzolanic action of silica fume at high temperatures. The compressive strength of normal cured UHPC at 28 days was in the range of 100–130 MPa.

None of the specimens subjected to heated curing showed a significant gain in strength after 7 days. The 7-day and 28-day strengths were almost identical. High curing temperature accelerates hydration reaction and material hardening, resulting in increased strength

at early ages.

8.2.4.1. 5Effect of steel fibers. It was observed that an increase in fiber content does not necessarily increase the compressive strength. For example, UHPC mix 11 (Table 6, CEM-III, SP-II, LSF) with 100 kg/m^3 of steel fibers yielded 160 MPa strength, whereas other mixes with higher fiber content failed at much lesser stress. Similar observations were made by Zhongke et al. [35] when a specimen with 2 % steel fiber exhibited 7 % higher strength compared to the specimen with 4 % fibers. Fibers in concrete bridge cracks and retard their propagation, therefore making concrete more ductile. Furthermore, the specimens without fibers were severely damaged by the sudden explosion. However, specimens incorporating steel fibers did not show any splitting or breakage into pieces after failure (Fig. 11).

8.3. Flexural strength

Fig. 12 presents the flexural strength results for UHPC, achieving a maximum flexural strength of 24 MPa and an average value of 18.7 MPa. At the initiation of each test, minute hairline cracks emerged at the base of the prism, with only a single main crack extending from the tension to the compression zone of the beam. Throughout the loading process, the UHPC beams with fibers remained intact, maintaining the steel fiber bond. At the point of peak load, the steel fibers began to pull out from the matrix at a specific location. The failure of UHPC beam specimens occurred due to the breakdown of the fiber-matrix bond, resulting in a significant increase in crack width, averaging 13 mm. Notably, there was no fiber rupture observed in any of the tests. The variation in flexural strength is ascribed to the differing homogeneity and porosity of the concrete matrix, influencing the fiber debonding effect. The results indicate that the inclusion of fibers markedly enhanced the flexural strength of the concrete. The steel fibers effectively bridged microcracks, resisting the development of macrocracks and preventing the specimens from splitting into two parts. All beams fractured within the middle third of the span, exhibiting a nearly vertical crack failure pattern. The modulus of rupture for UHPC was found to be up to five times higher than that of conventional concrete. These findings and observations align with those reported by other researchers [24].

8.4. Sulphate resistance

The test results (Table 8) reveal that an increase in the concentration of sulphate solution leads to a decrease in the compressive strength of UHPC specimens, with the reduction more pronounced at a 5 % concentration of sodium sulphate compared to a 1 % concentration. The compressive strength of the concrete specimens exhibited a consistent decline over the 56 days of exposure for both 1 % and 5 % concentrations of sodium sulphate. Specifically, reductions in compressive strength of 2 %, 2 %, 6 %, and 10 % were noted at 7, 14, 28, and 56 days of immersion, respectively, compared to the target strength. However, the compressive strength did not fall significantly below the target compressive strength of the mix. The minimal average loss of 5 % in compressive strength of UHPC after enduring severe sulphate exposure for 56 days underscores the increased resistance of the developed UHPC against sulphate attack. Consequently, the sulphate attack-related durability test indicates that the durability of the developed UHPC surpasses that of normal-strength concrete. This also suggests that the developed mixture possesses a very dense microstructure, resulting in negligible penetration of sulphate ions.

9. Conclusions

The experimental findings suggest that it is feasible to produce Ultra-High Performance Concrete (UHPC) with compressive strength reaching 160 MPa by utilizing local materials and conventional technology. The choice of raw materials, the mixing, and the curing regime play crucial roles in UHPC development. Mixes incorporating increased cement content, an optimized blend of sand, QP, SP, and steel fibers demonstrated enhanced workability and compressive strength. Mix 14 exhibited the greatest slump flow value, while mix 11 and the optimized mix demonstrated the highest compressive strengths. Employing heated curing resulted in higher strength compared to conventional room temperature curing. Notably, a 24 % increase in compressive strength was observed with the application of heated curing. In terms of cost (Table 9), ultra-high-performance concrete was found to be four times more expensive than normal-strength concrete, in contrast to commercially available UHPC, which is approximately 10 times more expensive than traditional concrete. Although this non-proprietary mix exhibits great potential, further testing is still needed to investigate its resistance against chloride environment and fatigue loading.

Data availability statement

Data generated during the experimentation of this manuscript has been included in this manuscript.

CRediT authorship contribution statement

Muhammad Azhar Saleem: Writing – original draft, Data curation, Conceptualization. **Faizan Liaquat:** Writing – review & editing, Methodology, Investigation. **Muhammad Mazhar Saleem:** Methodology, Investigation, Formal analysis. **Mubashir Aziz:** Writing – review & editing, Validation, Supervision, Investigation. **Fahid Aslam:** Writing – review & editing, Validation, Software,

(a)

(b)

Fig. 11. Modes of failure: (a) Cubes without fibers; and (b) Cubes with fibers.

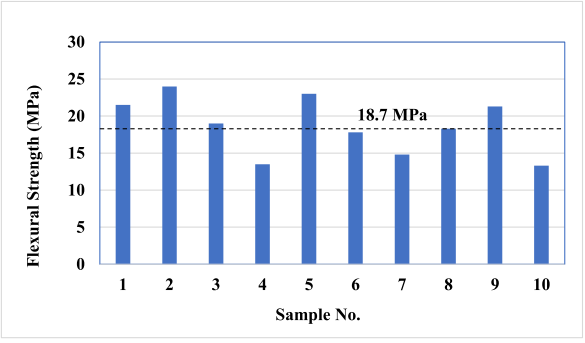

Fig. 12. Summary of flexural strengths for optimized mix.

Project administration. **Abdullah Mohamed:** Writing – review & editing, Resources, Funding acquisition, Data curation.

Declaration of generative AI and AI-assisted technologies in the writing process

During the preparation of this work the authors used ChatGPT in order to Rephrase some sentences. After using this tool/service, the authors reviewed and edited the content as needed and take(s) full responsibility for the content of the publication.

Declaration of competing interest

The authors declare that they have no known competing financial interests or personal relationships that could have appeared to influence the work reported in this paper.

Table 8
Reduction in length, mass and compressive strength of UHPC under sulphalte attack.

Exposure Solution (Na_2SO_4)	Duration (Days)	Length Reduction (%)	Weight Reduction (%)	Strength Reduction (%)
1 %	7th	0	0	3
		0	0	2
		0	0	1
1 %	14th	0	0	1
		1	0	0
		1	0	4
5 %	28th	2	0	8
		1	0	4
		0	0	7
5 %	56th	0	0	13
		1	0	8
		0	0	10
Average		1	0	5

Table 9
Cost analysis and comparison per cubic meter.

Material	Source	Rate (PkR)	Normal Strength Concrete		UHPC	
			Quantity (kg/m^3)	Amount (PkR)	Quantity (kg/m^3)	Amount (PkR)
Portland Cement	DG Khan	1100/bag	400	8800	800	17,600
Coarse Aggregates	Margala	148/cft	1077	3581	–	–
Fine Sand	Lawrencepur	110/cft	716	1754	429.3	1052
Silica Sand	Kamar Mishani	800/ton	–	–	429.3	343
Silica Fumes	BASF Chemicals	250/kg	–	–	232.5	58,125
Quartz Powder	Imporient Chemicals	125/kg	–	–	210	26,250
Super Plasticizer	Imporient Chemicals	130/kg	–	–	42.5	5525
Steel Fibers	Local Steel Wire (0.5 mm)	550/kg	–	–	150	82,500
Steel Bars (on average)	Mughal Steel	303/kg	100	30,300	–	–
Total (PkR)		–	–	44,435	–	1,91,395

Acknowledgments

This study is partially funded by the Future University in Egypt (FUE).

References

[1] C.M. Tam, V.W.Y. Tam, K.M. Ng, Assessing drying shrinkage and water permeability of reactive powder concrete produced in Hong Kong, Construct. Build. Mater. 26 (2012) 79–89.
[2] N. Van Tuan, G. Ye, K. van Breugel, A.L.A. Fraaij, B.D. Dai, The study of using rice husk ash to produce ultra high performance concrete, Construct. Build. Mater. 25 (2011) 2030–2035.
[3] A. Alsalman, C.N. Dang, W.M. Hale, Development of ultra high performance concrete with locally available materials, Development Ultra-High Perform. Concr. with Local. Available Mater. Constr. Build. Mater. 133 (2017) 135–145.
[4] R. Yu, P. Spiesz, H.J.H. Brouwers, Development of ultra-high performance fiber reinforced concrete (UHPFRC): towards an efficient utilization of binders and fibers, Construct. Build. Mater. 79 (2015) 273–282.
[5] R. Yu, L. van Beers, P. Spiesz, H.J.H. Brouwers, Impact resistance of sustainable ultra-high performance fiber reinforced concrete under pendulum impact loadings, Construct. Build. Mater. 107 (2016) 203–215.
[6] P. Richard, M.H. Cheyrezy, Reactive powder concrete, Cement Concr. Res. 25 (1995) 1501–1511.
[7] C. Wang, C. Yang, F. Liu, C. Wan, X. Pu, Preparation of ultra high performance concrete with common technology and materials, Cem. Concr. Compos. 34 (2012) 538–544.
[8] E.P. Sidodikromo, Z. Chen, M. Habib, Review of the cement-based composite ultra-high-performance concrete (UHPC), Open Civ. Eng. J. 13 (2019) 1.
[9] B.A. Graybeal, Compressive behavior of ultra-high-performance fiber-reinforced concrete, ACI Mater. J. 104 (2007) 2.
[10] M. Schmidt, E. Fehling, Ultra-high-performance concrete: research, development and application in Europe, ACI Spec. Publ. 228 (2005) 51–78.
[11] C. Gu, G. Ye, W. Sun, Ultrahigh performance concrete-properties, applications and perspectives, Sci. China Technol. Sci. 58 (2015) 587–599.
[12] E. Dong, R. Yu, D. Fan, Z. Chen, Absorption-desorption process of internal curing water in ultra-high performance concrete (UHPC) incorporating pumice: from relaxation theory to dynamic migration model, Cement Concr. Compos. 133 (2022) 104659.
[13] K. Liu, T. Yin, D. Fan, J. Wang, R. Yu, Multiple effects of particle size distribution modulus (q) and maximum aggregate size (Dmax) on the characteristics of Ultra-High Performance concrete (UHPC): experiments and modeling, Cement Concr. Compos. 133 (2022) 104709.
[14] D. Fan, W. Tian, R. Yu, Incorporation of liquid phase into solid particle packing model for precise design of low water/binder cement-based composites (LW/B-CC): modelling and experiments, Compos. B Eng. 242 (2022) 110070.
[15] J. Jiang, W. Zhou, H. Chu, et al., Design of eco-friendly ultra-high performance concrete with supplementary cementitious materials and coarse aggregate, J. Wuhan Univ. Technol.-Materials Sci. Ed. 34 (2019) 1350–1359, https://doi.org/10.1007/s11595-018-2198-4.
[16] J. Jinyang, Z. Wenjing, G. Yun, W. Liguo, W. Fengjuan, C. Hong-yan, X. Guangyuan, V. Brecht, S. Zeger, L. Jiabin, Feasibility of manufacturing ultra-high performance cement-based composites (UHPCCs) with recycled sand: a preliminary study, Waste Manag. 83 (2019) 104–112.
[17] H. Chu, Y. Zhang, F. Wang, T. Feng, L. Wang, D. Wang, Effect of graphene oxide on mechanical properties and durability of ultra-high-performance concrete prepared from recycled sand, Nanomaterials 10 (9) (2020) 1718, https://doi.org/10.3390/nano10091718.

[18] Q. Wang, H. Chu, W. Shi, et al., Feasibility of preparing self-compacting mortar via municipal solid waste incineration bottom ash: an experimental study, Archiv.Civ.Mech.Eng 23 (2023) 251, https://doi.org/10.1007/s43452-023-00794-5.
[19] K. Habel, J.-P. Charron, R.D.H. ShadiBraike, P. Gauvreau, B. Massicotte, Ultra-high performance fiber reinforced concrete mix design in central Canada, Can 35 (2008) 217–224.
[20] B.D. Weldon, D. V Jauregui, C.M. Newtson, C.W. Taylor, K.F. Montoya, S. Allena, Feasibility Analysis of Ultra High Performance Concrete for Prestressed Concrete Bridge Applications (No, NM0. 9, 2010.
[21] H.R. Sobuz, P. Visintin, M.M. Ali, M. Singh, M.C. Griffith, A.H. Sheikh, Manufacturing ultra-high performance concrete utilising conventional materials and production methods, Construct. Build. Mater. 111 (2016) 251–261.
[22] PS: 232, R)"Pakistan Standard Specification for Ordinary Portland Cement", Pakistan Standards and Quality Control Authority, 2008 n.d.
[23] A. C150, No Title, "Standard Specification for Portland Cement," n.d..
[24] B.A. Graybeal, Material Property Characterization of Ultra-high Performance Concrete, No. FHWA-HRT-0, 2006, pp. 6–103.
[25] A. C1611/1611m-14, No Title, "Standard Test Method for Slump Flow of Self-Consolidating Concrete," n.d..
[26] B.S.E.N. 12390-3, No Title, Compressive Strength of Test Specimens", Testing hardened concrete, 2001 n.d.
[27] Standard Astm C39, No Title, Test Method for Compressive Strength of Cylindrical Concrete Specimens", n.d..
[28] P. Dinakar, Design of Self-Compacting Concrete with Fly Ash, 2012, https://doi.org/10.1680/macr.10.00167.
[29] 2005 EFNARC, BIBM, CEMBUREAU, EFCA, ERMCO, The European Guidelines for Self-Compacting Concrete, 2005.
[30] M.Z.A.M. Zahid, B.H.A. Bakar, F.M. Nazri, H. Alasmari, M.F.P.M. Latiff, A. Ayob, K. Muhammad, M.M. Ahmad, B.H.A. Manaf, M.K. Ishak, Mechanical, durability and rheology properties of ultra high performance concrete (UHPC) with low cement content, IOP Conf. Ser. Earth Environ. Sci. 920 (2021), https://doi.org/10.1088/1755-1315/920/1/012005.
[31] A.K. Akhnoukh, C. Buckhalter, Ultra-high-performance concrete: constituents, mechanical properties, applications and current challenges, Case Stud. Constr. Mater. 15 (2021) e00559, https://doi.org/10.1016/j.cscm.2021.e00559.
[32] H.J. Chen, Y.L. Yu, C.W. Tang, Mechanical properties of ultra-high performance concrete before and after exposure to high temperatures, Materials 13 (2020) 1–17, https://doi.org/10.3390/ma13030770.
[33] P.P. Li, Q.L. Yu, H.J.H. Brouwers, Effect of PCE-type superplasticizer on early-age behaviour of ultra-high performance concrete (UHPC), Construct. Build. Mater. 153 (2017) 740–750, https://doi.org/10.1016/j.conbuildmat.2017.07.145.
[34] S. Li, S. Cheng, L. Mo, M. Deng, Effects of steel slag powder and expansive agent on the properties of ultra-high performance concrete (UHPC): based on a case study, Materials 13 (2020) 1–11, https://doi.org/10.3390/ma13030683.
[35] Z. Sun, S. Yang, M. Hang, J. Wang, T. Yang, Optimization design of ultrahigh-performance concrete based on interaction analysis of multiple factors, Case Stud. Constr. Mater. 16 (2022) e00858, https://doi.org/10.1016/j.cscm.2021.e00858.
[36] M. Ding, R. Yu, Y. Feng, S. Wang, F. Zhou, Z. Shui, X. Gao, Y. He, L. Chen, Possibility and advantages of producing an ultra-high performance concrete (UHPC) with ultra-low cement content, Construct. Build. Mater. 273 (2021) 122023, https://doi.org/10.1016/j.conbuildmat.2020.122023.
[37] A. Alsalman, C.N. Dang, J.R. Martí-Vargas, W. Micah Hale, Mixture-proportioning of economical UHPC mixtures, J. Build. Eng. 27 (2020), https://doi.org/10.1016/j.jobe.2019.100970.
[38] M. Azeem, M. Azhar Saleem, Role of electrostatic potential energy in carbon nanotube augmented cement paste matrix, Construct. Build. Mater. 239 (2020) 117875, https://doi.org/10.1016/J.CONBUILDMAT.2019.117875.
[39] M. Azeem, M. Azhar, Hydration model for the OPC-CNT mixture : theory and experiment, Construct. Build. Mater. 264 (2020) 120691, https://doi.org/10.1016/j.conbuildmat.2020.120691.
[40] M. Azeem, M.T. Junaid, M. Azhar, Correlated strength enhancement mechanisms in carbon nanotube based geopolymer and OPC binders, Construct. Build. Mater. 305 (2021) 124748, https://doi.org/10.1016/j.conbuildmat.2021.124748.
[41] Y. Chen, P. Liu, F. Sha, J. Yin, S. He, Q. Li, Z. Yu, H. Chen, Study on the mechanical and rheological properties of ultra-high performance concrete, J. Mater. Res. Technol. 17 (2022) 111–124, https://doi.org/10.1016/j.jmrt.2021.12.139.